

An Automated Framework for Lithium Battery State of Health (SOH) Analysis

Vinicius Matheus B. Pereira^{*}, Janisley Oliveira De Sousa[†], Gustavo Couto Fonseca[‡], Ricardo Nogueira Santos[§]

Sidia Institute of Science and Technology, Manaus, Brazil

Email: {^{*}vinicius.pereira, [†]janisley.sousa, [‡]gustavo.fonseca, [§]ricardo.santos}@sidia.com

Abstract—In this paper, we explore the capacity degradation mechanisms inherent to lithium batteries within consumer electronics, specifically focusing on the repercussions of fast charging techniques on the State of Health (SOH). We present an innovative automation framework tailored to oversee and control the charging and discharging cycles of these batteries under various C-rate scenarios. Experiments were carried out in a controlled testbed demonstrating the framework's proficiency in analyzing the battery's SOH degradation rate. Lithium-ion polymer (LiPo) batteries were used for experimental validation. Our results indicate a significant correlation between higher C-rates and accelerated battery degradation, with a 2.58% decrease in SOH observed at 3C over 30 cycles, demonstrating that a 3C charging profile degrades the SOH by 15% more than a 0.5C profile. These results show the importance of balancing fast charging capabilities with the overall longevity of lithium battery systems. Consequently, our research affirms the potential of the proposed framework as a valuable tool for in-depth studies on diverse lithium-based battery technologies.

Index Terms—Lithium-ion polymer (LiPo) battery, Fast charging, State of Health (SOH), Capacity degradation, Calendar aging

I. INTRODUCTION

Nowadays, battery performance is one of the most critical issues faced in the consumer electronics industry, mainly for mobile phones that are essential for many quotidian tasks. Users expect the battery to last for long hours, accompanied by accurate indications of remaining charge time before recharging becomes necessary. Lithium-ion polymer (LiPo) batteries, renowned for their high energy density, minimal memory effect, and low self-discharge, have become the most widely used batteries in consumer devices such as smartphones and tablets [1] [2]. Despite all the advantages of using Lithium-ion batteries, they are likely to suffer from issues caused by aging, with capacity degradation being the primary concern. Moreover, an exhausted battery causes negative feelings on user experience and in some extreme cases leads to unexpected shutdowns. As a result, several studies have been carried out to investigate the influence of different factors on lithium-ion battery consumption and its useful lifetime [3].

Lithium-ion polymer batteries are prevalent in numerous portable electronic devices due to their substantial energy capacity and low self-discharge [4]. However, It's crucial to avoid overheating or overcharging lithium-ion polymer batteries to prevent damage that could result in hazardous

or explosive outcomes [5]. In the aging process, battery usable capacity gets reduced along the charging cycles, the degradation occurs due to various mechanisms such as Solid Electrolyte Interphase (SEI) formation and dissolution, thermal runaway, and Li-plating [4] [5]. Aging is accelerated by high current consumption, high charging current, overheating, and so on [5]. To enhance customer satisfaction, the industry has embraced faster charging methods, which can expedite battery health deterioration [6] [7]. Most fast charging methods are based on high charging current values, which increase battery temperature and energy loss due to the internal resistance of the cell. Additionally, higher currents will favor side reactions and hence capacity will degrade at a higher rate [8].

In this scenario, extensive research has been undertaken to devise charging profiles for Lithium-based batteries that enable fast charging without adversely impacting the SOH. Such advancements could serve as a distinguishing commercial advantage among competing brands [6]. Many of the recommended charging methods employ a multistage profile, where a substantial amount of the battery's State of Charge (SoC) is achieved using a high, steady charging current [9]. This observation has primarily driven our focus toward the constant current (CC) stage. However, despite their widespread use, there remains a gap in understanding the long-term effects of the CC stage on battery health, highlighting the need for more thorough research.

The primary focus of this study is to introduce a novel automated framework for evaluating the SOH of lithium battery technologies. We investigate the effects of constant current charging profiles on battery degradation, crucial for optimizing fast charging processes in lithium batteries. Our experiments utilized LiPo batteries under Constant Current and Constant Voltage (CC-CV) conditions. This framework is designed to efficiently evaluate and monitor the capacity degradation and performance of lithium-based batteries over prolonged periods.

The paper is organized as follows: Section II discusses the background on the SOH of lithium-based batteries. In Section III, we show the experimental methodology used in this work. The proposed framework for battery SOH analysis is implemented in Section IV. Section V presents results evaluating the performance of the proposed framework. Finally, Section VI presents the conclusions and future research directions.

II. BACKGROUND

A. Battery Technologies

Although some mature battery technologies are available in the electronics industry including lead-acid, Ni-Cd, and Ni-MH, for contemporary applications, lithium-based batteries have emerged as the major standard. Representing a significant advancement over Ni batteries, Lithium batteries offer several advantages, including a higher energy storage density, lightweight properties, a typical voltage of 3.7V, reduced risk of bursting, and a prolonged lifespan over multiple recharging cycles [12].

Lithium batteries can be classified according to the electrolyte construction: liquid or polymer. The traditional liquid electrolyte is composed of substances such as diethyl carbonate, ethylene carbonate, or dimethyl carbonate. In contrast, the polymer electrolyte is formulated using a high-conductivity gel infused with lithium salts [13]. Transitioning from liquid to polymer electrolytes presents several advantages in smartphone production, including the feasibility of designing thin and customized shapes [13].

B. Charging Methods

Energy can be transferred to batteries through various methods. While these processes cause stress on the internal components and affect the aging process, the overall battery lifespan is intrinsically linked to the chosen transfer technique, as discussed in Section I.

The majority of charging approaches are based on CC-CV strategies. In the CC method, a steady current is injected, whereas in the CV method, the battery terminals are consistently maintained at a specified voltage. Ayoub [14] presented a review of charging methods, a brief summary is shown in Table I.

TABLE I
STANDARD BATTERY CHARGING METHODS

Method	Strategy
Trickle charge and CC-CV	Charge in three stages. Trickle charge injects a small current. Only necessary when battery voltage is under 3V. CC until Vbat reaches a threshold. CV while current higher than a minimum. Most frequently used method.
Five-step charging	Repeats CC stages under different and smaller current.
Pulse charging	Based on pulse-width modulation.
Boost charging	Based on CC-CV technique. A high current (Iboost) is injected during a time (Tboost).

C. Battery SOH Estimation Methods

The aging effect on batteries is inherently tied to the chemical properties of the lithium-ion (Li-ion) material, which leads to a degradation in battery capacity over time [15]. A common metric found in the literature to gauge battery performance over its lifespan is the State of Health. The SOH measures a battery's remaining capacity relative to its original capacity [16]:

$$SOH(i) = \frac{C(i)}{C0} * 100\%$$

Where:

$C(i)$ represents the battery's capacity at the i charging cycle, $C0$ denotes the battery's original capacity when new.

The decline in SOH for Li-ion and LiPo batteries is due to irreversible chemical processes. These processes impact the internal components of the battery, leading to changes in the electrode material phase, variations in the electrode's dynamic performance, and alterations in the electrolyte's decomposition state [17]. Yao [17] graphically depicts these chemical processes in Fig. 1.

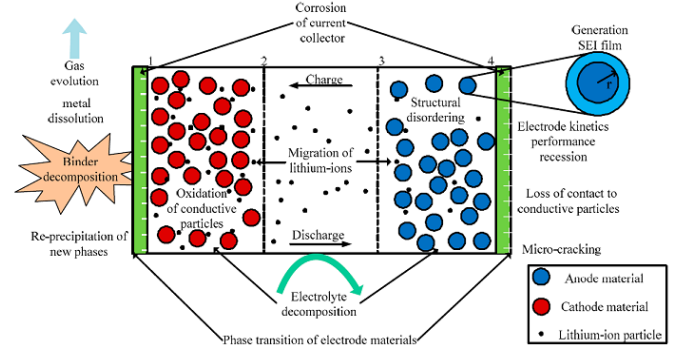


Fig. 1. Chemical battery degradation [17]

Battery degradation is directly impacted by various factors including age, charging/discharging cycles, power, temperature, and operational severity. Baidan [18] categorized battery aging into two main primary mechanisms: calendar and cycle aging, such processes are shortly described in Table II.

TABLE II
MAIN BATTERY AGING DEGRADATION MECHANISMS

Mechanism	Characteristic
Calendar aging	Degradation associated with the storage time. Degradation even without charging cycles. May be reverted, depending on the storage time.
Cycle aging	Rated: Degradation at nominal charging/discharging current. Battery is discharged over 70-80% in each cycle. May be reverted, depending on the storage time.
	Harsh: Degradation under variable conditions (Out of the nominal current range, temperature, depth of discharge, charging/discharging intensity, Cut-off voltage and charging methods).

For safe battery operation, accurate SOH estimation is crucial, once a battery undergoes significant degradation, it should be decommissioned to prevent hazardous conditions [19]. According to Baydan [18] and Nuroldayeva [20], SOH estimation methods are divided into two main categories: model-based and experimental. Model-based methods determine SOH through fundamental battery characteristics such as current and voltage. After validating the model experimentally, SOH can be deduced from these characteristics [20].

Experimental methods typically demand sophisticated equipment to gather basic battery data throughout charge and discharge cycles, which can be time-consuming. These experiments provide insights into battery aging behavior over these cycles [21]. In literature, experimental SOH estimation is usually bifurcated into direct and indirect methods. Based on the works of Baydan [18] and Nuroldayeva [20], the methods and theoretical foundations are presented in Table III.

TABLE III
EXPERIMENTAL SOH ESTIMATION METHODS

	Type	Theoretical basis
Direct	Internal resistance [22]	Equivalent resistance circuit.
	Electrochemical impedance spectroscopy [23]	Frequency response analyser applying CV or CC.
	Cycle counting [24]	Charging and discharging cycles submitted.
	Coulomb counting [25]	Based on current integration.
Indirect	Incremental capacity analysis [26]	Ratio of increasing capacity to differential voltage.
	CC-CV charging [27]	Charging data curve.
	Differential voltage analysis [28]	Differential voltage curve analysis.
	Ultrasonic [29]	Ultrasonic waves.

III. METHODOLOGY

A. Experimental Setup

The research's experimental setup is illustrated in Fig. 2. The setup employs a Keithley precision DC Supply and a Battery Simulator, model 2281S-20-6, to control the charging and discharging cycles of the batteries. Keithley simulator is managed by a Python algorithm executed on a personal computer, supplying the LiPo battery with CC-CV charging method while it is being charged and acting as the battery's constant current supply during discharging. The SOC is estimated using the Coulomb Counting method, as implemented in the Keithley simulator by integrating the battery's current flow.

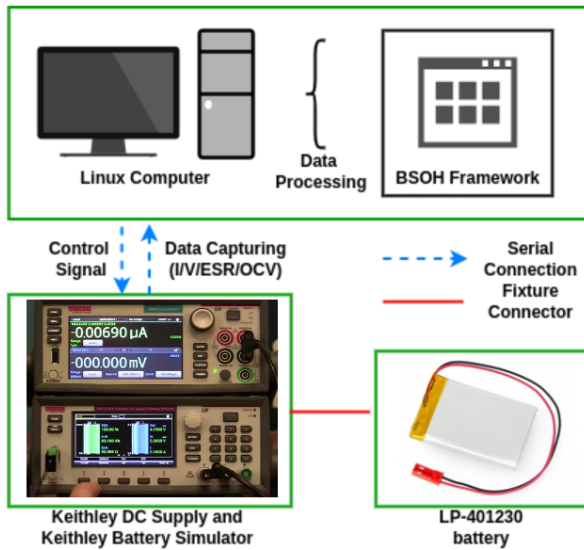


Fig. 2. Experimental setup for battery SOH analysis

The battery chosen in this work is a LiPo battery with 105mAh of nominal capacity, commonly used in electronic consumer devices. LiPo battery consists of a lithium-ion cell that uses a high conductivity gelled polymer electrolyte instead of the popular liquid electrolyte, keeping the same electrode reactions. The battery-rated performance is shown in table IV. The charging and discharging processes adhere to the following conditions: a standard charge, discharge at a rate of 0.2C down to 3.5V, a rest period of 30 minutes between charge/discharge cycles, and continuation until the discharge capacity is less than 60%. Under these conditions, the battery manufacturer ensures a battery lifespan of over 500 cycles.

TABLE IV
THE NOMINAL SPECIFICATIONS OF LP-401230 BATTERY

Item	Specification
Technology	Lithium-polymer
Capacity	105mAh
Charging voltage	4.2V
Voltage at end of discharge (EoD)	3.0V
Nominal voltage	3.7V
Standard charge	Constant current: 0.2C Constant voltage: 4.2V Cut-off current: 0.01C
Fast charge	Constant current: 1C Constant voltage: 4.2V Cut-off current: 0.01C
Standard discharge	Constant current: 0.2C Cut-off voltage: 3.0V
Maximum continuous discharge current	1C
Operation temperature range	Charge: 0 to 45°C Discharge: -20 to 60°C
Life expectancy	500 cycles

Using the experimental setup shown in Fig. 2, we performed the experiments on 10 batteries tailored to each specific C-rate variation (0.5C at 50mA, 1C at 100mA, and 3C at 300mA). These experiments employed a CC-CV charging method and a CC discharging method at 50mA, discharging to a level of 3.5V, as shown in Fig. 3.

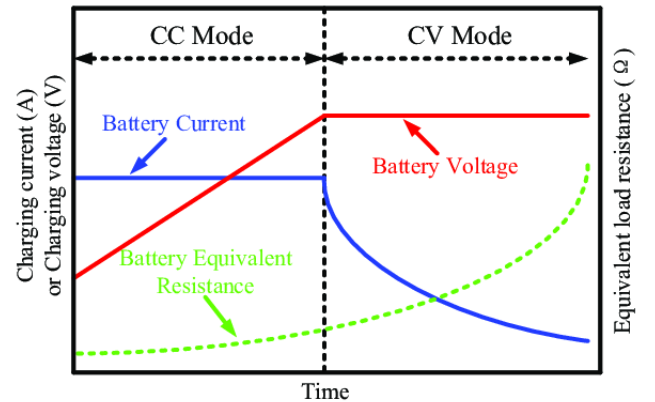


Fig. 3. CC-CV charging method [30]

All initial parameters, including voltage and current levels, protections, and sampling rate, were predetermined at the

beginning of the experiments. Each experiment was designed to capture the nuances of battery performance degradation and behavior under the stipulated conditions.

B. Experiment Procedure

The battery capacity degradation experiment via cycling aging is structured to obtain insights into the battery's behavior under diverse charging conditions. Here is a breakdown of the established experiment procedure:

1) Equipment calibration process:

- We ensure that all instruments are precisely calibrated to the requisite thresholds, guaranteeing the fidelity of measurements. The requirements are:
 - Set the Over Current Protection (OCP) at 500mA.
 - Set the Over Voltage Protection (OVP) at 4.3V.

2) Charging process:

- Set the voltage threshold for end-of-charging (V_{set}) at 4.2V.
- Test under varying C-rates (0.5C, 1C and 3C).

3) Discharging process:

- Perform a standard discharge at a rate of 0.5C, equivalent to 50mA.
- Adhere to a cut-off voltage (V_{cutoff}) of 3.5V during the discharge phase.

IV. THE LITHIUM BATTERY SOH FRAMEWORK

The core of this study is the battery State of Health framework, meticulously designed to automate the measurement of charge/discharge cycles and gauge battery capacity degradation. The implementation employs the Python programming language to control the Keithley simulator using Standard Commands for Programmable Instruments (SCPI). Utilizing the Pyvisa library, we automated crucial tasks such as setting the calibration process, configuration values for the battery, managing charge/discharge cycles, and executing data acquisition. Moreover, protection mechanisms are enabled to prevent scenarios like overcharging, undercharging, and short circuits, thereby safeguarding the battery and equipment integrity. Also, initial equipment calibrations are conducted to set parameters like voltage, current levels, protections, thresholds, and the sampling rate.

After the calibration process, the automated framework operates in two phases. During the first phase, the battery is charged using the CC-CV method, where the charging current is maintained constant until the specified voltage threshold is reached in the CC phase, after which the charging voltage is maintained constant until the charging rate falls below a specified threshold in the CV phase. In the second phase, the battery is discharged using only the CC method, which maintains a constant current over time. Both phases operate in a controlled environment, as defined in Section III.

Algorithm 1 delineates the procedure for charging cycles during the first stage. Initially, the instrument's sample rate is adjusted to 7ms, with a provision for OCP at 500mA and OVP at 4.3V. Subsequently, Equivalent Series Resistance

(*ESR*) and Open Circuit Voltage (*OCV*) are measured, and the charging is initiated using the CC-CV charging method, setting the final battery voltage to 4.2V and cut-off current (I_{cutoff}) to 1mA. Data, extracted every second, is transmitted to the computer. Upon reaching the end current, the charging is ceased and a log report is generated writing charging data in a file. After that, the framework is prepared for the initiation of the discharging cycle.

Algorithm 1 Algorithm for charging

```

1: OpenLogfile() && OpenInstrumentConnection();
2: Set sample rate to 7ms;
3: Set protections:  $OCP = 500mA$ ,  $OVP = 4.3V$ ,  $V_{set} = 4.2V$ ,  $I_{cutoff} = 1mA$ ;
4: Measure ESR and OCV;
5: Start CC-CV charging method;
6: while (InstrumentOutputIsOn() is TRUE) do
7:   Access instrument every 1s;
8:   Read Voltage, Current and SoC;
9:   Stop charging when  $I_{cutoff}$  is reached;
10: end while
11: WriteDataToLogfile() && LogFinalMeasurements();
12: PrepareInstrumentforDisch();

```

Algorithm 2 describes the procedure for discharging cycles during the second phase. Initially, the instrument's sample rate and protective measures are established. Then, *ESR* and *OCV* are quantified, and the voltage is set to the *OCV*. A calibration function is initiated to determine the battery discharging voltage (V_{set}) required to achieve the discharging current (I_{dch}) equal to 50mA. Discharging process starts, with data sampling of 1s, coupled with periodic adjustments to maintain the I_{dch} at a steady 50mA. When the battery voltage (V_{bat}) reaches 3.5V, discharging is finished. Finally, discharging logs are stored in a log report.

Algorithm 2 Algorithm for discharging

```

1: OpenLogfile() && OpenInstrumentConnection();
2: Set sample rate to 7ms;
3: Set protections:  $OCP = 500mA$ ,  $OVP = 4.3V$ ;
4: Measure ESR and OCV;
5: Set  $V_{set} == OCV$  && StartCalibrationCycle();
6: Adjust  $V_{set}$  until ( $I_{dch} = 50mA$ );
7: Start CC method for discharging;
8: while ( $I_{dch} < 50mA$ ) do
9:   Access instrument every 1s;
10:  Check  $V_{set} = V_{set} - 1mV$ ;
11:  Read Voltage, Current and SoC;
12:  Stop discharging when  $V_{bat} = 3.5V$ ;
13: end while
14: WriteDataToLogfile() && LogFinalMeasurements();
15: TurnOffInstrument();

```

V. EXPERIMENTAL RESULTS AND DISCUSSION

In this section, we evaluate the effectiveness of our proposed framework for analyzing lithium batteries' SOH. While data collected in a laboratory setting is insulated from external noise, on-device data may be affected by variables such as temperature changes and device activities. To demonstrate the robustness of our approach in real-world scenarios, we conducted experiments on batteries in a controlled testbed using the CC-CV charging algorithm outlined in section III.

A. Temperature Variance

Given the fact that the battery's temperature can rise above the ambient room temperature during the testbed experiments, we segmented our temperature analysis into two distinct phases: before and after the charging process. This was achieved by capturing thermal images of the battery surface. Fig. 4a displays the image taken prior to initiating the charging experiments, showing temperatures ranging between 23°C and 25°C . Upon completing the charging process, subsequent thermal images were captured. Fig. 4b, Fig. 4c, and Fig. 4d illustrate the battery surface temperatures corresponding to the charging currents of 0.5C, 1C, and 3C, respectively.

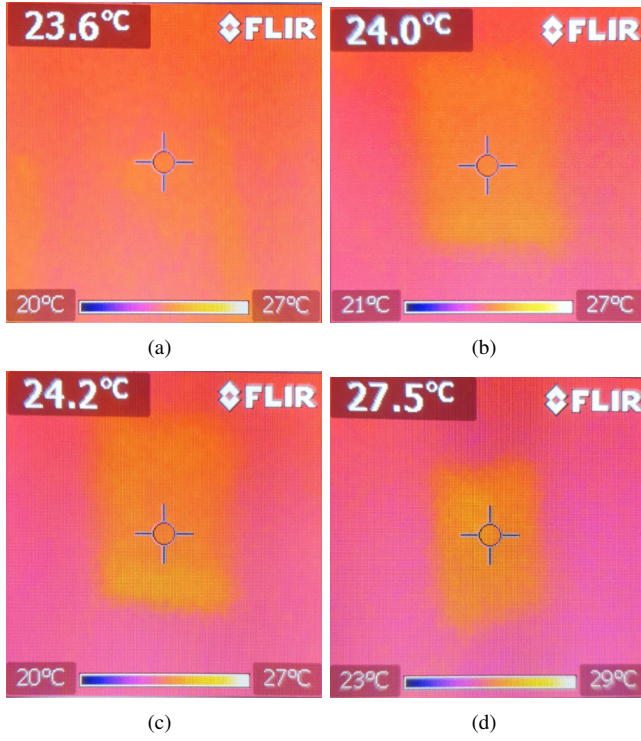


Fig. 4. (a) Initial battery temperature before charging. (b) Battery charging temperature with 0.5C (c) Battery charging temperature with 1C (d) Battery charging temperature with 3C

Charging the battery at these high C-rates resulted in an increase in temperature of 3.9°C and a reduction in the battery's energy storage capacity. To ensure the health and safe operation of LiPo batteries, it's crucial to maintain a stable temperature. Therefore, we allow the battery a rest period of 30 minutes between charging and discharging cycles.

Moreover, during the experiments, the charging current is decreased and the cut-off voltage is adjusted whenever the temperature ventures outside of the designated safe ranges. In environments with elevated ambient temperatures, the charging voltage exhibits a more pronounced positive correlation with SOH degradation.

B. CC and CV modes

During the CC phase, the current was held constant. As shown in Fig. 5, as C-rates increased from 0.5C to 3C, the duration of the CC charging also increased: by 3.83% for 0.5C, 3.74% for 1C, and 2.69% for 3C. This increase can be attributed to battery degradation after 30 cycles, resulting in a reduced absolute EoD. Meanwhile, Fig. 6 illustrates a decrease in CV mode as the number of battery cycles increased.

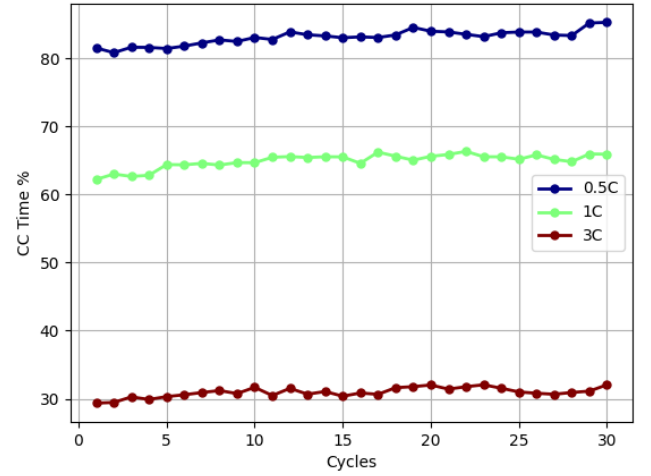


Fig. 5. CC time variation along cycles increases

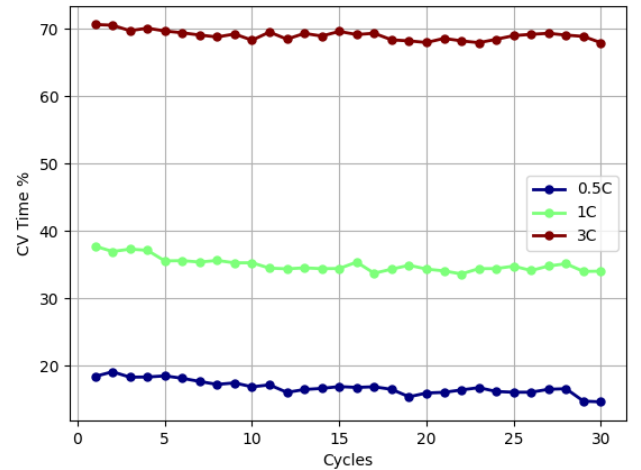


Fig. 6. CV time variation along cycles increases

In our study, we closely examined the duration of the CC-CV charging process, which is crucial for the battery's SOH. With the CC charging step finished, the voltage is maintained at a stable level while the amount of the current is reduced to reach the cut-off level and attend the full battery charged step. The CV time was reduced by 3.77% for 0.5C, 3.72% for 1C and 2.69% for 3C. Consequently, the full charge voltage threshold was decreased as a consequence of reduced SOH.

Both CC and CV modes significantly contribute to battery degradation, as observed in our study. During the CC phase, despite the current being consistent, an increase in C-rates resulted in prolonged CC charging times, indicating battery degradation. Specifically, after 30 cycles, the CC charging time increased due to diminished EoD. In the subsequent CV phase, where the voltage is stabilized while the current is tapered to achieve a full charge, the duration decreases with more battery cycles. This reduction in CV time is a direct consequence of the declining SOH, ultimately leading to a lowered full charge voltage threshold. Collectively, these observed trends underscore the intricate relationship between the CC and CV modes and their compounded effects on battery degradation.

C. Charging and Discharging time

The charging and discharging processes are crucial for analyzing battery SOH, with factors such as maximum voltage, Depth of Discharge (DoD), current, load profiles, and temperature significantly affect the rates of capacity loss. Fig. 7 highlights the benefits of high C-rates in reducing the full-charging time. For 0.5C, 1C, and 3C, the End-of-Charge (EoC) time decreased by 4.88%, 5.90%, and 9.51% respectively. However, charging at high C-rates can diminish the battery's energy storage capacity and its ability to consistently deliver power, consequently impacting its SOH.

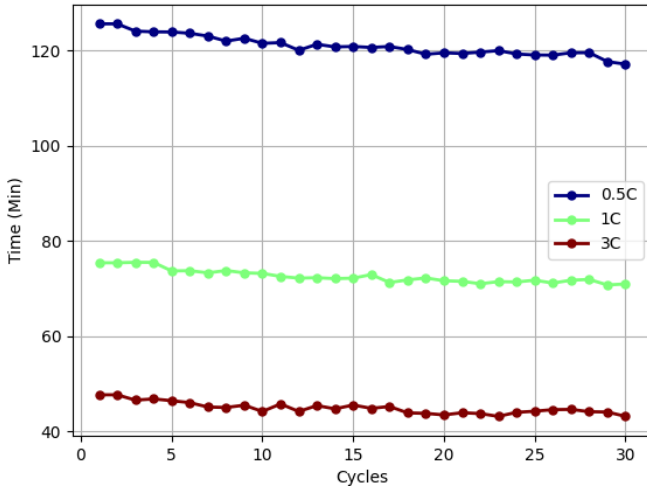


Fig. 7. Battery charging time profiles

Fig. 8 shows the LiPo battery's reduced lifespan across discharge cycles. The End-of-Discharge (EoD) time decreased by 2.45% for 0.5C, 2.62% for 1C, and 2.81% for 3C. This

reduction is associated with battery degradation caused by imbalances in current, temperature variations, and material stress, factors that can lead to battery swelling and accelerate cell breakdown due to constraints in LiPo intercalation and diffusion.

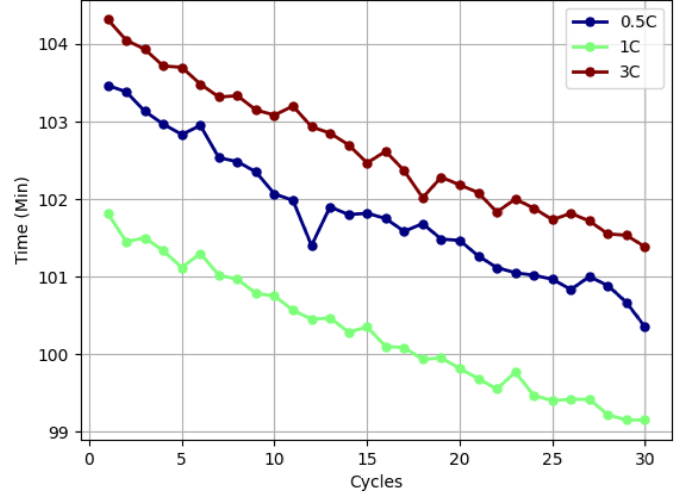


Fig. 8. Battery discharging time profiles

D. Average Charging Current

To evaluate the effectiveness of increasing the C rate in reducing the overall charging time, we calculated the average charging current. This was achieved by dividing the total charging capacity by the comprehensive CC-CV charging method duration required for each C-rate, as depicted in Fig. 9.

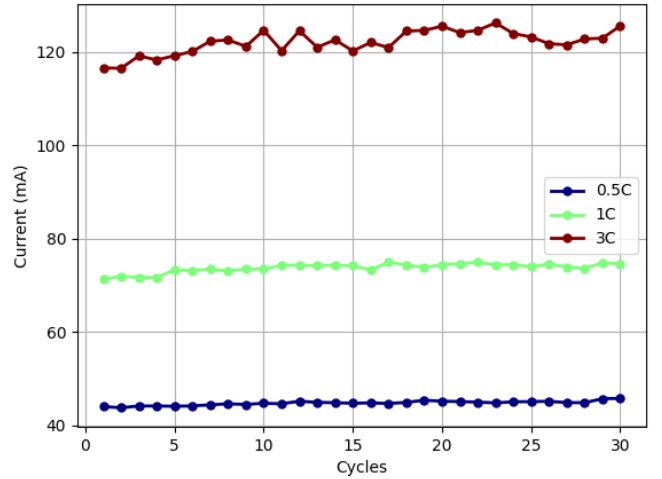


Fig. 9. Average charging current according to cycles variation

From the data in Fig. 9, we can see that the battery's potential to exploit high C-rates is limited by its design capacity. At a 0.5C charging rate, the recorded average charging current after 30 cycles was 45.73mA, closely aligning with the expected 50mA. For the 1C rate, the 30-cycle average

was 74.56mA, reflecting a 25% decrease from the CC phase. Meanwhile, at 3C, the end average charging current measured 125.55mA, which is below half the designated CC current for that parameter. Furthermore, a clear pattern emerges with an increase in the average charging current as the cycle count goes up, indicating battery degradation. This rise is directly related to the prolonged CC charging time observed in earlier results.

The implications of increased average charging currents are particularly evident when considering the measured C-rates. At a 0.5C rate, the battery experiences minimal deviation from the expected current, indicating manageable stress and heat generation. However, at higher rates like 1C and especially 3C, the effects become more pronounced. The substantial decrease in efficiency at these rates, with a 25% reduction at 1C and even greater at 3C, highlights the accelerated degradation due to the higher stress and heat on the battery's chemical components. These conditions not only lead to reduced efficiency but also increase safety risks and significantly shorten the battery's lifespan. Such high charging currents, while enabling faster charging, come at the cost of the battery's overall health and longevity, making it crucial to balance the need for quick charging with the long-term implications on battery performance and safety.

E. SOH degradation

The LiPo batteries were fully charged and discharged repeatedly for 30 cycles. The battery SOH percentage was obtained in each cycle in comparison to the first cycle, as shown in Fig. 10.

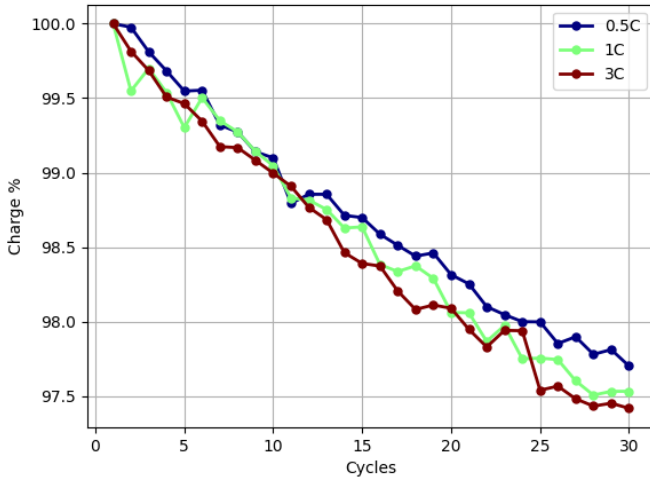


Fig. 10. SOH degradation after 30 battery cycles

From the data obtained, it was observed an SOH degradation of 2.29% for 0.5C, 2.46% for 1C, and 2.58% for 3C, confirming the direct relationship between high C-Rates and a worse battery degradation over time. These results reaffirm a crucial trade-off in lithium-ion polymer battery technology: while high C-rates can accelerate the charging process by

reducing the duration of CC mode, they inevitably impact the battery's longevity and health. Therefore, manufacturers and users need to find a delicate balance between the appeal of fast charging and the overarching goal of extended battery life. Additionally, these results confirm the ability of the proposed automated framework to accurately analyze battery SOH.

F. Adaptive Framework Design

The efficacy of the proposed battery SOH analysis framework is closely tied to its adaptability across varying battery characteristics and operational conditions. The algorithms delineated encapsulate a systematic approach for SOH assessment through controlled charging and discharging cycles. Yet, their flexibility to adjust to diverse battery parameters remains essential. Vital parameters, such as the sampling rate, protection thresholds, and end currents for charging, coupled with targeted discharge currents and voltage calibrations for discharging, highlight the framework's versatility.

The framework is intrinsically modular, making it adaptable to various lithium battery chemistries and operational environments. This design underscores its prowess in consistently delivering optimal charging/discharging recommendations and thorough battery SOH assessments. Its versatility extends to encompass multiple lithium-based battery technologies.

VI. CONCLUSION

This study introduces an automated framework for assessing the State of Health (SOH) of lithium batteries under various charging conditions. Using the proposed framework, this study evaluated the impact of higher C-rates on the charging time of Li-Po battery technology. The findings indicate degradation of 2.58% in the battery's SOH at 3C over 30 cycles, demonstrating that a 3C charging profile degrades the SOH by 15% more than a 0.5C profile. Additionally, charging the battery at these high C-rates resulted in a temperature increase of 3.9°C and a reduction in the battery's energy storage capacity. These results validate the framework's proficiency in accurately assessing SOH degradation, and they highlight the effect of charging profiles on battery capacity degradation patterns, as detailed in Section V. The framework monitors key battery parameters, thereby ensuring safe operating conditions during the charging and discharging processes.

The experiments conducted using the proposed automated framework demonstrated a marked capacity reduction in batteries under fast charging compared to standard charging methods. This accelerated degradation, driven by the intricate interaction of thermal dynamics and increased internal resistance, underscores the effectiveness of our framework in analyzing the SOH of lithium batteries. Our comprehensive analysis, centered on this framework, provides vital insights into the SOH of lithium batteries under various charging conditions.

Further research is warranted to compare the outcomes of battery capacity degradation through extended charging cycle testing across different lithium-based battery technologies.

ACKNOWLEDGMENT

The authors are grateful for the support offered by the SIDIA R&D Institute in the Model project. This work was partially supported by Samsung, using resources of Informatics Law for Western Amazon (Federal Law No. 8.387/1991). Therefore, the present work disclosure is in accordance as foreseen in article No. 39 of number decree 10.521/2020.

REFERENCES

- [1] X. Zhang and C. Mi, *Vehicle power management: modeling, control and optimization*. Springer Science and Business Media, 2011.
- [2] J. Yang, X. Li, X. Sun, Y. Cai, and C. Mi, "An efficient and robust method for lithium-ion battery capacity estimation using constant-voltage charging time," *Energy*, vol. 263, p. 125743, 2023.
- [3] N. Noura, L. Boulon, and S. Jemei, "A review of battery state of health estimation methods: Hybrid electric vehicle challenges," *World Electric Vehicle Journal*, vol. 11, no. 4, p. 66, 2020.
- [4] T. Kim, W. Song, D.-Y. Son, L. K. Ono, and Y. Qi, "Lithium-ion batteries: outlook on present, future, and hybridized technologies," *Journal of materials chemistry A*, vol. 7, no. 7, pp. 2942–2964, 2019.
- [5] P. V. Chombo and Y. Laoonual, "A review of safety strategies of a Li-ion battery," *Journal of Power Sources*, vol. 478, p. 228649, 2020.
- [6] M. Xu, B. Reichman, and X. Wang, "Modeling the effect of electrode thickness on the performance of lithium-ion batteries with experimental validation," *Energy*, vol. 186, p. 115864, 2019.
- [7] C.-C. Chang, S.-Y. Huang, and W.-H. Chen, "Thermal and solid electrolyte interphase characterization of lithium-ion battery," *Energy*, vol. 174, pp. 999–1011, 2019.
- [8] W. Xie et al., "Challenges and opportunities toward fast-charging of lithium-ion batteries," *Journal of Energy Storage*, vol. 32, p. 101837, 2020.
- [9] G.-L. Zhu et al., "Fast charging lithium batteries: recent progress and future prospects," *Small*, vol. 15, no. 15, p. 1805389, 2019.
- [10] R. Fu, S.-Y. Choe, V. Agubra, and J. Fergus, "Development of a physics-based degradation model for lithium-ion polymer batteries considering side reactions," *Journal of Power Sources*, vol. 278, pp. 506–521, 2015.
- [11] Y. Gao, X. Zhang, Q. Cheng, B. Guo, and J. Yang, "Classification and review of the charging strategies for commercial lithium-ion batteries," *Ieee Access*, vol. 7, pp. 43511–43524, 2019.
- [12] M. Singh, J. Trivedi, P. Maan, and J. Goyal, "Smartphone Battery State-of-Charge (SoC) Estimation and battery lifetime prediction: State-of-art review," in *2020 10th International Conference on Cloud Computing, Data Science and Engineering (Confluence)*, 2020, pp. 94–101.
- [13] Y. Liang et al., "A review of rechargeable batteries for portable electronic devices," *InfoMat*, vol. 1, no. 1, pp. 6–32, 2019.
- [14] E. Ayoub and N. Karami, "Review on the charging techniques of a Li-Ion battery," in *2015 Third International Conference on Technological Advances in Electrical, Electronics and Computer Engineering (TAECE)*, 2015, pp. 50–55.
- [15] M. Kassem, J. Bernard, R. Revel, S. Pelissier, F. Duclaud, and C. Delacourt, "Calendar aging of a graphite/LiFePO₄ cell," *Journal of Power Sources*, vol. 208, pp. 296–305, 2012.
- [16] J. Sivaranjani, B. Sandeep, V. R. Olety, and N. Karanth, "Intelligent charging system for dedicated applications using lithium ion battery," in *2016 Online International Conference on Green Engineering and Technologies (IC-GET)*, 2016, pp. 1–7.
- [17] L. Yao et al., "A review of lithium-ion battery state of health estimation and prediction methods," *World Electric Vehicle Journal*, vol. 12, no. 3, p. 113, 2021.
- [18] S. S. Baydan, M. Ceylan, and R. N. Tuncay, "A Study on the State of Health of Lithium-ion Batteries," in *2021 13th International Conference on Electrical and Electronics Engineering (ELECO)*, 2021, pp. 509–513.
- [19] R. Zhou, S. Fu, and W. Peng, "A review of state-of-health estimation of lithium-ion batteries: Experiments and data," in *2020 Asia-Pacific International Symposium on Advanced Reliability and Maintenance Modeling (APARM)*, 2020, pp. 1–6.
- [20] G. Nuroldayeva, Y. Serik, D. Adair, B. Uzakbaiuly, Z. Bakenov, and others, "State of Health Estimation Methods for Lithium-Ion Batteries," *International Journal of Energy Research*, vol. 2023, 2023.
- [21] M. Elmahallawy, T. Elfouly, A. Alouani, and A. Massoud, "A Comprehensive Review of Lithium-Ion Batteries Modeling, and State of Health and Remaining Useful Lifetime Prediction," *Ieee Access*, 2022.
- [22] J. Sihvo, T. Roinila, T. Messo, and D.-I. Stroe, "Novel online fitting algorithm for impedance-based state estimation of Li-ion batteries," in *IECON 2019-45th Annual Conference of the IEEE Industrial Electronics Society*, 2019, vol. 1, pp. 4531–4536.
- [23] L. A. Middlemiss, A. J. Rennie, R. Sayers, and A. R. West, "Characterisation of batteries by electrochemical impedance spectroscopy," *Energy Reports*, vol. 6, pp. 232–241, 2020.
- [24] K. N. Akpinar, B. Gundogdu, and O. Ozgonenel, "A novel cycle counting perspective for energy management of grid integrated battery energy storage systems," *Energy Reports*, vol. 9, pp. 123–131, 2023.
- [25] B. Zine, H. Bia, A. Benmouna, M. Becherif, and M. Iqbal, "Experimentally validated coulomb counting method for battery state-of-charge estimation under variable current profiles," *Energies*, vol. 15, no. 21, p. 8172, 2022.
- [26] X. Li, C. Yuan, X. Li, and Z. Wang, "State of health estimation for Li-Ion battery using incremental capacity analysis and Gaussian process regression," *Energy*, vol. 190, p. 116467, 2020.
- [27] J. Yang, X. Li, X. Sun, Y. Cai, and C. Mi, "An efficient and robust method for lithium-ion battery capacity estimation using constant-voltage charging time," *Energy*, vol. 263, p. 125743, 2023.
- [28] L. Wang, C. Pan, L. Liu, Y. Cheng, and X. Zhao, "On-board state of health estimation of LiFePO₄ battery pack through differential voltage analysis," *Applied Energy*, vol. 168, pp. 465–472, 2016.
- [29] Y. Wu, Y. Wang, W. K. Yung, and M. Pecht, "Ultrasonic health monitoring of lithium-ion batteries," *Electronics*, vol. 8, no. 7, p. 751, 2019.
- [30] S.-H. Hwang, Y. Chen, H. Zhang, K.-Y. Lee, and D.-H. Kim, "Reconfigurable hybrid resonant topology for constant current/voltage wireless power transfer of electric vehicles," *Electronics*, vol. 9, no. 8, p. 1323, 2020.